NANYANG TECHNOLOGICAL UNIVERSITY SINGAPORE

Regulating arrival UAV flows between the AirMatrix and the droneport using a dynamic carousel circuit

Yixi Zeng, Gregoire Ky, and Vu N. Duong

Air Traffic Management Research Institute
Nanyang Technological University, Singapore

Date: 9th Dec 2021

Agenda

1) Background and problem statement
2) Concepts
   - Droneport
   - Dynamic carousel circuit
3) Research framework
4) Methodology
   1) Simulation
   2) Optimization model
5) Results
6) Conclusion

Background

- The rise of drone operations
- Potential hazards of drone operations in urban area
  - Safety issue (during approach, landing, and takeoff phases)
  - Airspace congestion issue
- Infrastructure for approach and departure drones

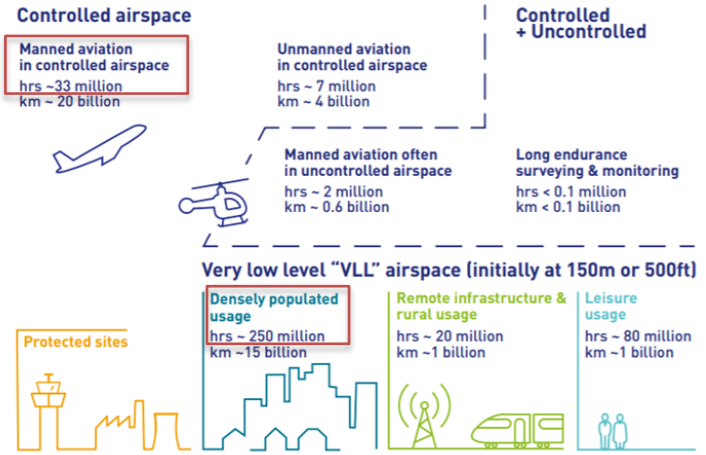

Figure 1: Impact on Airspace of manned vs. unmanned operations (statistic estimated by SESAR) [1]

[1] G. Rohit, Nov 2018. [Online]. Available:https://ntrs.nasa.gov/api/citations/20190001472/downloads/20190001472.pdf

Background

- The rise of drone operations

- Potential hazards of drone operations in urban area
  - Safety issue (during approach, landing, and takeoff phases)
  - Airspace congestion issue

- Infrastructure for approach and departure drones

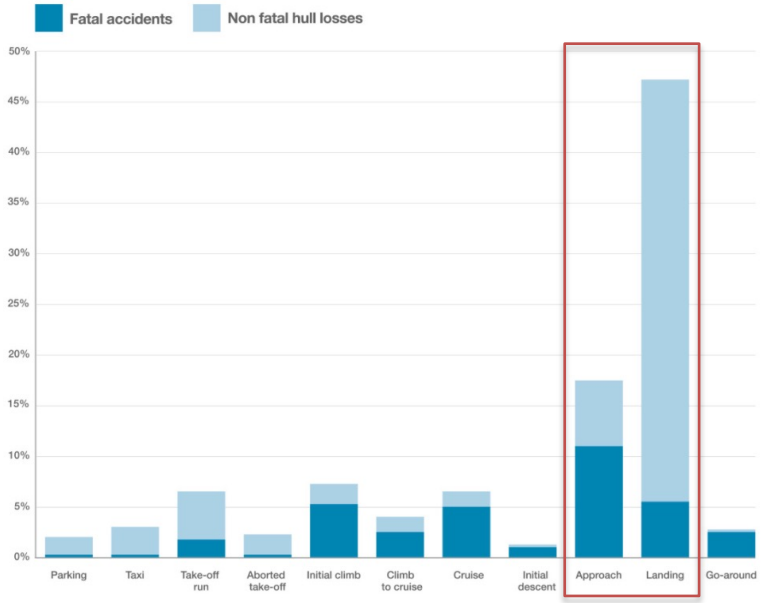

Figure 2: Accidents by flight phase as a percentage of all accidents (1999-2019) [2]

[2] A. S. Airbus, 2020. [Online]. Available: https://accidentstats.airbus.com/statistics/accident-by-flight-phase

Background

- The rise of drone operations

- Potential hazards of drone operations in urban area
  - Safety issue (during approach, landing, and takeoff phases)
  - Airspace congestion issue

- Infrastructure for approach and departure drones

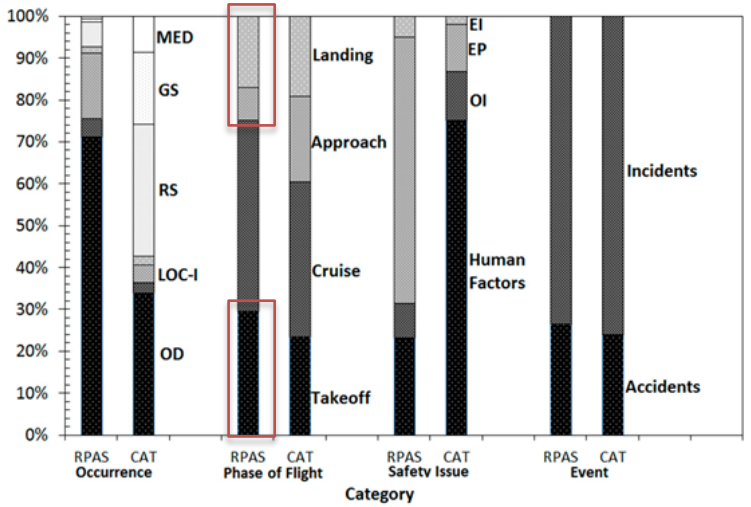

Figure 3: Distribution of accidents and incidents of Remotely Piloted Aircraft System (RPAS) vs. commercial air transportation [3]

[3] G. Wild, J. Murray, and G. Baxter, "Exploring Civil Drone accidents and incidents to help prevent potential air disasters," Aerospace, vol. 3, 2016.

Background

- The rise of drone operations
- Potential hazards of drone operations in urban area
  - Safety issue (during approach, landing, and takeoff phases)
  - Airspace congestion issue
- Infrastructure for approach and departure drones

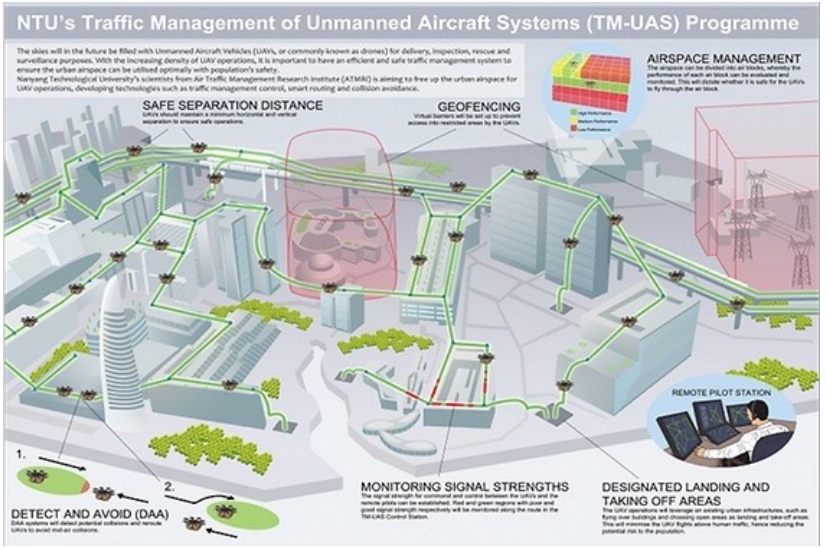

Figure 4: ATMRI's TM-UAS illustration [4]

How can we provide the secure use of low-altitude airspace during approach and departure phases, for a wide range of applications of drones?

[4] W. Dai, B. Pang, and K. H. Low, "Accessibility analysis of unmanned aerial vehicles near airports with a four-dimensional airspace management concept," in 2020 AIAA/IEEE 39th Digital Avionics Systems Conference (DASC), 2020, pp. 1–9.

Droneport

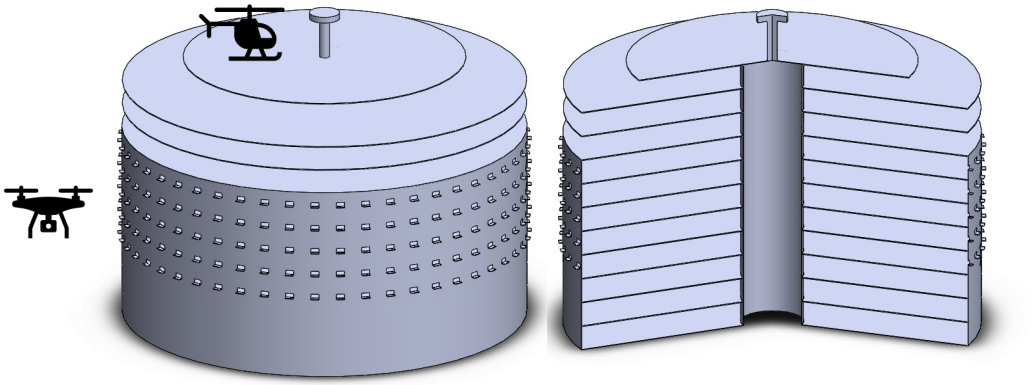

Figure 5: Droneport illustration

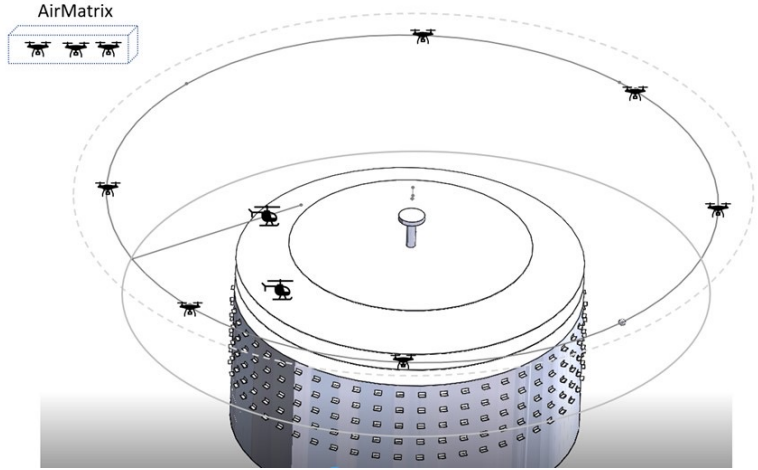

Figure 6: Carousel circuit surrounding the droneport

[4] W. Dai, B. Pang, and K. H. Low, “Accessibility analysis of unmanned aerial vehicles near airports with a four-dimensional airspace management concept,” in 2020 AIAA/IEEE 39th Digital Avionics Systems Conference (DASC), 2020, pp. 1–9.

Dynamic Carousel Circuit

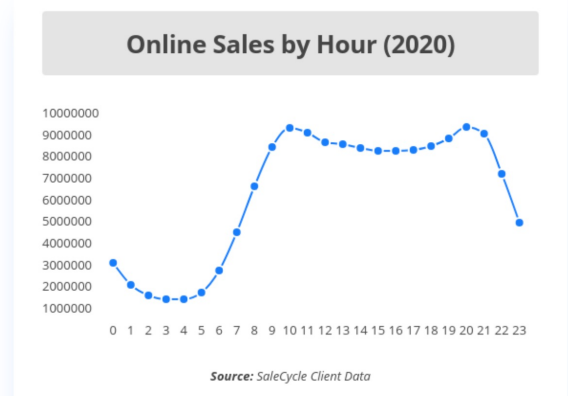

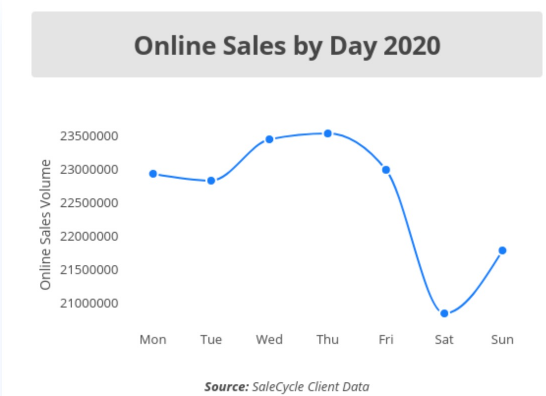

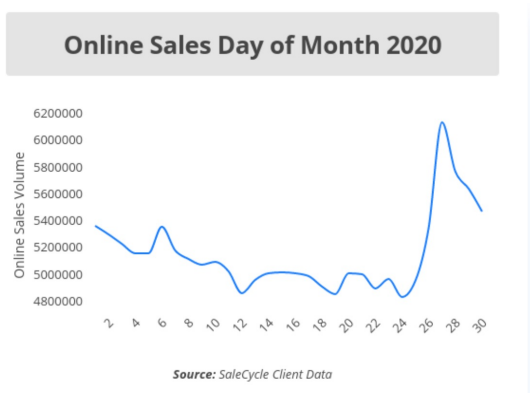

Higher demand → Larger capacity → Larger carousel circuit

[5] "When Are People Most Likely to Buy Online? - SaleCycle", *SaleCycle*, 2021. [Online]. Available: https://www.salecycle.com/blog/stats/when-are-people-most-likely-to-buy-online/. [Accessed: 26- Jan- 2021].

Research framework

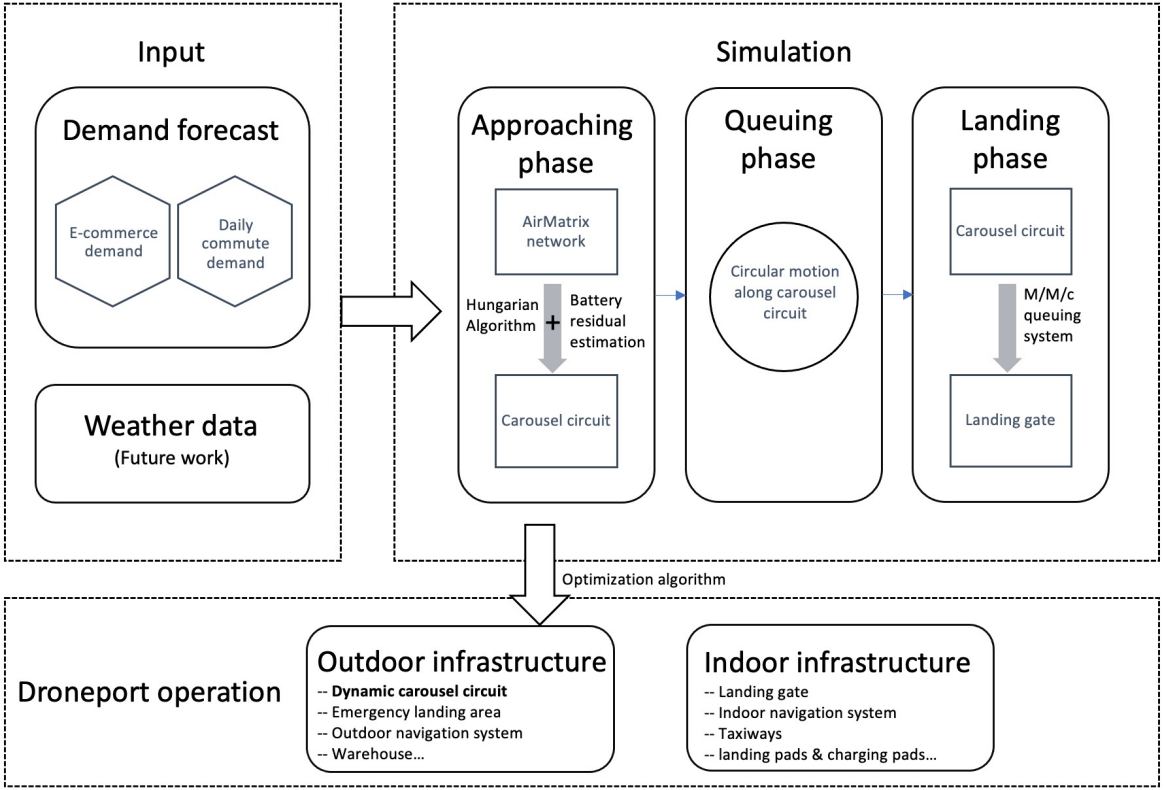

Simulation

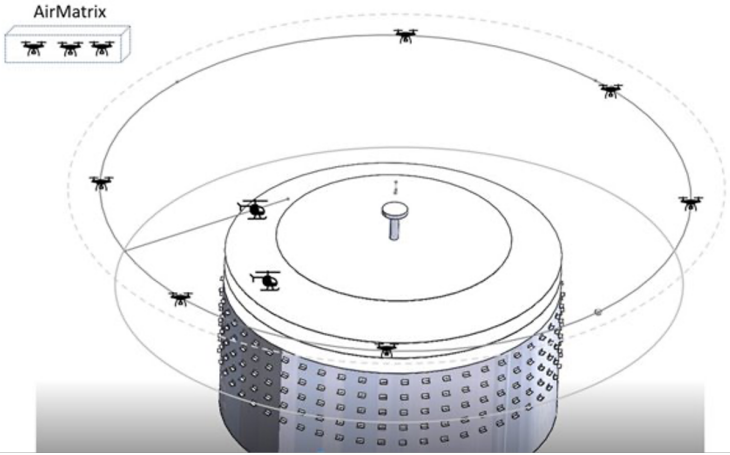

Figure 6: Carousel circuit surrounding the droneport

1. Initialization

   Generating the arrival time, the assigned landing gate, and the residual battery level that follow a Poisson process, random generation, and a normal process respectively

$$\left\{\left(t^a_{v,l}, G_v, B'_{v,l}\right)\right\}_{v=1}^{V_e}, \tag{1}$$

$$t^a_{(v+1),l} = t^a_{v,l} + u_{(v+1)}, \tag{2}$$

$$G_v = n, n \in N_g. \tag{3}$$

2. Approaching phase

   The mainstream of traffic is from the AirMatrix. The drone will approach the droneport in the same orientation as its assigned landing gate.

Simulation

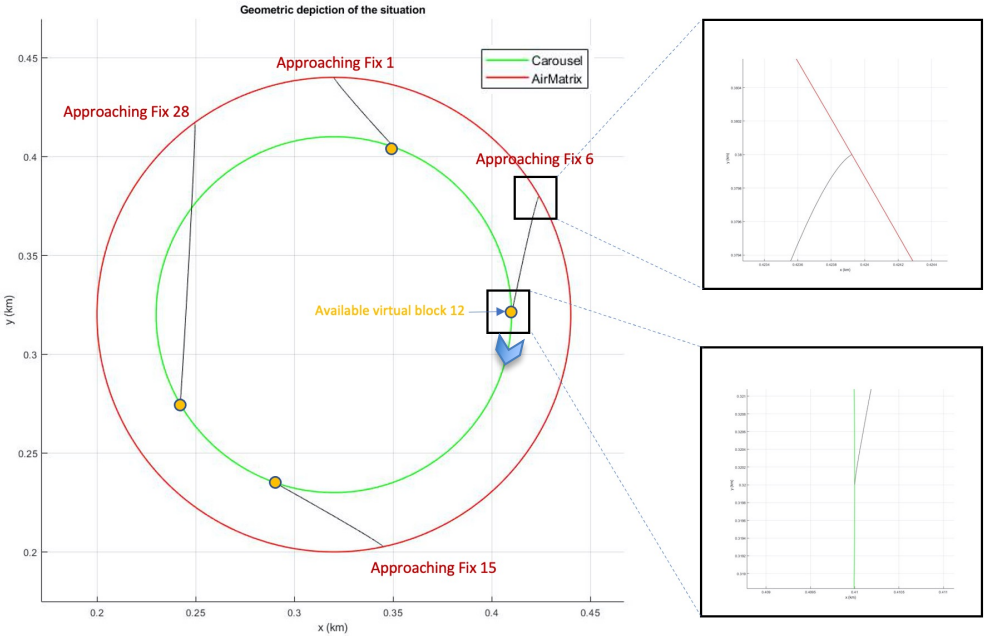

Figure 7: Top-down view of the cubic trajectory from the approaching fix point 6 on the AirMatrix to the metering fix point 12 on the carousel circuit.

2. Approaching phase

This phase selects available virtual blocks to the approaching drones from the AirMatrix and minimizes the total travel time and the battery consumption. Hungarian algorithm is implemented to solve this assignment problem.

$$H(t) = \begin{bmatrix} h_{11} & h_{12} & \cdots & h_{1Y} \\ h_{21} & h_{22} & \cdots & h_{2Y} \\ \vdots & \vdots & \ddots & \vdots \\ h_{X1} & h_{X2} & \cdots & h_{XY} \end{bmatrix} = [h_{xy}], \quad (4)$$

$$h_{xy} = \tau_{xy} + B_x^{'}, \quad (5)$$

$$x = N_v^{'}(t)(1), N_v^{'}(t)(2), ...N_v^{'}(t)(X), \quad (6)$$

$$y = N_b^{'}(t)(1), N_b^{'}(t)(2), ...N_b^{'}(t)(Y), \quad (7)$$

$$N_v^{'}(t) = \{\{v, l\}, l \in N_a : \alpha_l^v(t) = 1, \forall v \in V_a\}, \quad (8)$$

$$N_b^{'}(t) = \{j \in N_b : \alpha_j^v(t) = 0, \forall v \in V_a\}. \quad (9)$$

Simulation

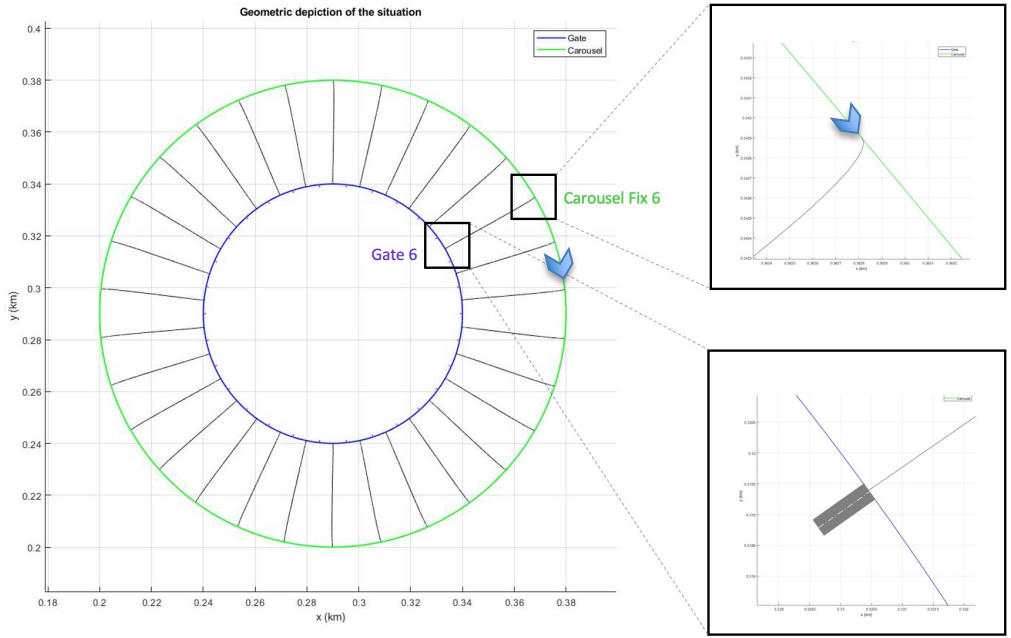

3. Queuing phase

   The carousel circuit acts as an approaching pattern to reduce the collision risk.

4. Landing phase

   Each landing gate is equipped with a simple M/M/c queuing system, which has c servers with arrivals following a Poisson process and service times observed to be an exponential distribution.

Figure 8: Geometric depiction of the cubic trajectory from the metering fix Point 6 on the carousel circuit to the landing Gate 6.

Simulation

5. Residual endurance estimation model

A residual endurance estimation model is developed based on the model designed by Hwang et al. [9].

The capability of this model is expanded to calculate the residual endurance of a multirotor UAV with the remaining battery level as an input.

Algorithm 1: Drone endurance estimation

Data: Battery voltage drop gradient k, nominal battery capacity C_0, fully charged voltage V_0, standard voltage V_s, rated discharge time t_0, Peukert's coefficient p, discharge rate λ.
Input : Current residual battery level b_0
Input : Forward flight speed U
Output: Remaining endurance t_b

Initialization;
Current voltage: $V_1 = b_0 * (V_0 - V_s) + V_s$;
Initial required current: $I_1 = \frac{P_{re}}{V_1}$;
Current capacity: $C_1 = C_0 - \frac{V_0 - V_1}{k}$;
Required propulsion power $P_{re} = power(U)$ (*power* function is developed based on multirotor drone aerodynamic.);

while *capacity error* $> \epsilon$ **do**
  $t_b = (i-1) * timestep\ (i = 1, 2, 3, 4, ...)$;
  // Calculate the decreased battery voltage
  $V_{i+1} = V_0 - k * (C_0 - C_i)$;
  // Calculate the required current
  $I_{i+1} = \frac{P_{re}}{V_{i+1}}$;
  // Calculate the actual available capacity
  $C_{i+1} = t_0^{1-p} * C_0^p * (I_{i+1}^{1-p} - I_1^{1-p}) + C_1 - \sum_{n=2}^{i+1} I_n * timestep$;
  // Calculate the error *capacity*
  $error = (C_{i+1} - (1-\lambda) * C_0)/((1-\lambda) * C_0)$;
end

[6] M.-H. Hwang, H.-R. Cha, and S. Jung, "Practical endurance estimation for minimizing energy consumption of multirotor unmanned aerial vehicles,"Energies, vol. 11, p. 2221, 08 2018.

Optimization Model

Output: optimum circuit radius, flight speed along the carousel circuit, and circuit altitude.

Constraints:

- All the drones from the AirMatirx network can join the carousel circuit without hovering above the droneport airspace. The value of fail means the number of drones that are not assigned to any available virtual blocks during approaching phase.
- The remaining battery levels of the landed drones B'_r are higher than 5%.

Objective function

$$\min \sum_{v \in V_e} \tau_{v,lm_v} + \tau_{v,m_v m_g} + \tau_{v,m_g n} + \beta \cdot \left(B'_{v,lm_v} + B'_{v,m_v m_g} + B'_{v,m_g n} \right)$$

$$\text{s.t. } \text{fail} = 0,$$

$$B'_r > 5\%.$$

Results

Table I. Important parameters employed in the simulation

(a)

Parameter	Symbol	Value	Units
Time separation	t_s	3	sec
Landing gate service time	t_g	1	sec
flight speed (phase 1, 3)	U_{al}	10	m/s
AirMatrix altitude	h_a	70	m
Landing gate altitude	h_g	40	m
Total arriving drones	D	5000	
Nominal capacity	C_0	32000	mAh
Rated discharge time	T_0	0.2	hr
Battery voltage drop gradient	k	1.2	
Fully charged voltage	V_0	49	V
Standard voltage	V_s	22.2	V
Peukert's coefficient	p	1.05	
Discharge fraction	λ	0.7	

Peak hour demand: 14360

3-level circuit

Arrival rate used in simulation: 5000

Table II. Simulation results under different arrival rates

(b)

	Arrival rates (drones/hr)	Circuit radius (m)	Flight speed (m/s)	Altitude (m)	Fails
Optimized →	5000	70.709	3.0039	12.804	0
	5000	60	3	12	921
	6000	70.709	3.0039	12.804	0
	7000	70.709	3.0039	12.804	467

+12835 s

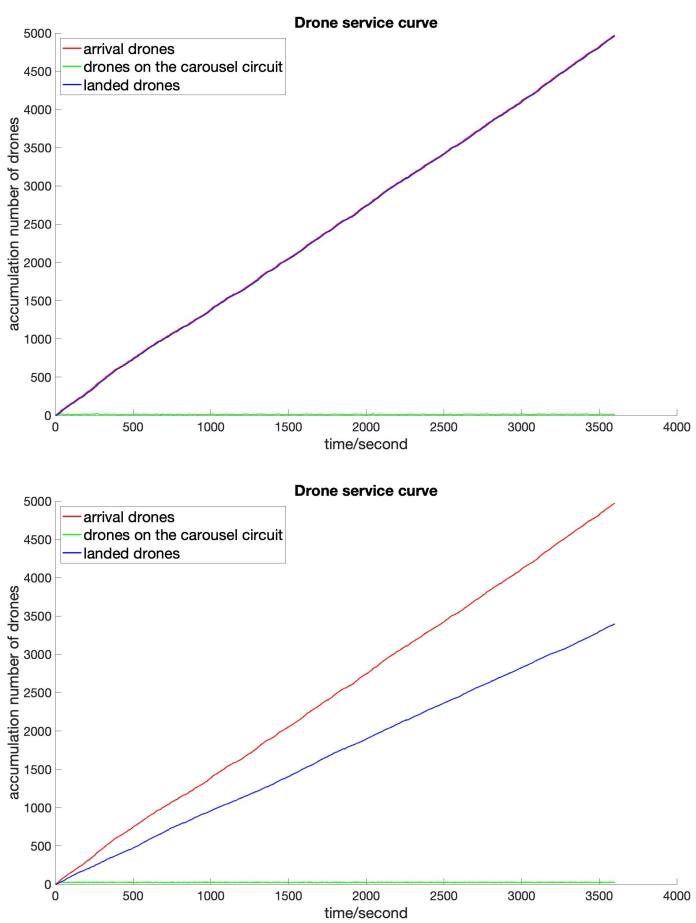

Figure 9. The drone service curve (a) with optimized dynamic carousel circuit; (b) without optimized dynamic carousel circuit.

Conclusion

- Droneport
  - a service facility providing a safe operation environment for heterogeneous drones
  - diverging from a recent trend, the design of droneport focused more on air traffic control and regulation enforcement
- Dynamic carousel circuit
  - act as a traffic pattern that manages drones coming in and coming out of the droneport
  - adjustable radius based on predicted demand
- Carousel circuit simulation model
  - equipped with a residual endurance estimation model and cubic trajectory planning
  - able to find an optimum circuit radius according to current demand

Future work

- Multi-level and multi-lane circuits with transition rules applied between each level
- Weather uncertainty

Q&A

Regulating arrival UAV flows between the AirMatrix and the droneport using a dynamic carousel circuit

Yixi Zeng
zeng0117@e.ntu.edu.sg

Gregoire Ky
ga.ky@ntu.edu.sg

Vu N. Duong
vu.duong@ntu.edu.sg